Simulation Analysis and Experimental Study on the Effect of Valve Opening on Flow Measurement Based on Micro-channel

Xin-ju Fu[1,2(✉)], Ping Wang[1,2], Yong Li[1,2], Zhao-xin Shi[1,2], Xu-dong Wang[1,2], and Tai-zeng Lv[1,2]

[1] Beijing Institute of Control Engineering, Beijing 100190, China
oranged1113@126.com
[2] Beijing Engineering Research Center of Efficient and Green Aerospace Propulsion Technology, Beijing 100190, China

Abstract. Thermal mass flow controllers use capillary tubes to form fluid channels. For microfluidic channel smaller than 1 mm, in the supercritical state, the pressure difference between the inlet and the outlet is large, resulting in obvious changes in fluid density. At the same time, the increase of the pressure gradient will cause the fluid cannot reach the fully developed stage of flow quickly. Therefore, in the flow analysis and heat transfer analysis, the microfluidic channel is quite different from the conventional scale channel. Based on the 0.34 mm capillary microfluidic channel, this paper analyzes the influence of the downstream valve opening on fluid flow and heat transfe. It can be seen from the simulation analysis and experimental data that the larger the opening of valve is, the lower the back pressure of the capillary channel is. Due to the accelerating state of fluid, the fully developed convective heat transfer and incompressible flow state are damaged, thereby affecting the real-time flow measured by the heating wire wrapped around the capillary.

Keywords: Thermal mass flow controller · Microfluidic channel · Valve opening · Flow measurement

1 Introduction

Thermal mass flow controller uses capillaries wrapped with heating wires to form fluid channels. Power on the heating wire, and measure the change of temperature field caused by gas flow to achieve real-time flow measurement. By adjusting the opening of the proportional valve at the downstream of the capillary to realize the flow control function [1, 2]. According to the principle of heat conduction, the thermal mass flow controller directly measures the mass flow of the fluid by using the heat exchange between the flowing fluid and the external heating source. It is suitable for micro-flow measurement, with the characteristics of small pressure loss, small volume and high reliability, and has been widely used in petroleum, chemical, medical food and other industries [3, 4]. In recent years, with the development of aerospace technology, space science exploration

L. Yan and J. Na (Eds.): ICFPMCE 2022, AHE 10, pp. 317–332, 2023.
https://doi.org/10.2991/978-94-6463-022-0_28

missions such as gravitational wave detection, gravitational gradient measurement, and deep space exploration have put forward urgent needs for high-precision flow controllers. The micro flow controller provides the accurate parameters of system working medium to realize fast and accurate closed loop control of thrust [5, 6].

When designing the flow controller, the capillary is designed according to the measured flow range. When the diameter of the capillary is less than 1 mm, it belongs to the micro-scale fluid channel, which is quite different from the conventional-scale channel in flow analysis and heat transfer analysis. For example, when the flow controller is applied to the propulsion subsystem of spacecraft, the upstream pressure is high and the downstream pressure is close to vacuum, so the large pressure difference between the upstream and downstream makes the fluid density change more obvious, which cannot be simply simplified as an incompressible fluid for analysis.

At the same time, when the opening of the downstream proportional valve is different, the back pressure changes and then the fluid velocity changes, which has a great impact on the precise measurement of micro flow. Therefore, it is necessary to analyze and study this phenomenon in the process of developing the flow controller.

2 Controller Design

As shown in Fig. 1, the flow controller is composed of a flow sensor, a current diverter, a flow regulating valve and a conditioning circuit. The principle is to transmit the analog signal on the flow sensor that changes with the flow to the conditioning circuit for signal conditioning. By calculating the real-time flow, comparing this flow with the set flow, and then amplifying the difference signal to control the regulating valve, the closed-loop control of the flow is realized.

According to the flow calculation formula [7]:

Subcritical state:

$$G = C_d f_1 Pi \sqrt{\frac{2k}{RT(k-1)}} \times \sqrt{\left(\frac{P_e}{P_i}\right)^{\frac{2}{k}} - \left(\frac{P_e}{P_i}\right)^{\frac{k+1}{k}}} \tag{1}$$

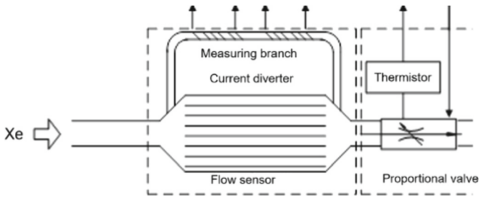

Fig. 1. Schematic Diagram of Flow Controller

Supercritical and critical state:

$$G = C_d f_I Pi \sqrt{\frac{2k}{RT(k+1)}} \times \left(\frac{2}{k+l}\right)^{\frac{1}{k-1}} \tag{2}$$

Definition:
G—Mass flow through valve, kg/s;
C_d—Flow coefficient, according to the flow coefficient test curve (Gas);
$f1$—Throttle area, m^2;
Pi—Inlet pressure, Pa;
Pe—Outlet pressure, Pa;
R—Gas constant, J/kg · K, for Xe: $R = 63.5$J/kg · K;
T—Absolute temperature, K;
k—Adiabatic index, for Xe: k = 1.67.
Critical pressure ratio:

$$\varepsilon_c = \left(\frac{2}{k+1}\right)^{\frac{k}{k-1}} = 0.487 \tag{3}$$

Since the outlet pressure Pe of the flow controller is close to vacuum, therefore:

$$\left(\frac{pe}{pi}\right) << 0.487 \tag{4}$$

It belongs to the supercritical working state. For the supercritical working state, according to Eq. (2), for a specific fluid medium, after the flow controller structure, inlet pressure Pi, and fluid temperature T are all determined, it can be seen that the mass flow through is determined by the valve port area f1. So we can obtain the required flow by adjusting the proportional valve to change the valve port area.

The core part of the flow controller is the flow sensor, which is based on the principle of thermally distributed mass flow measurement and is usually used for the micro flow measurement [8, 9]. A typical thermal capillary structure is used as the gas measurement unit, which consists of a circular thin-walled capillary and self-heating dual winding heating wires wrapped on it. Both windings have heating and temperature measurement functions, and they can be heated to 110 °C after power-on. When there is airflow, the cold gas reduces the coil temperature. The temperature difference between the upstream coil and the flow is the largest, so the coil is cooled more; The downstream coil is much less cooled by gas. As a result the average temperature of the downstream coil is higher than that of the upstream coil [10].

There are two basic working principles of the above thermal distributed flow measurement, one is constant temperature difference, the other is constant power. The constant temperature difference measurement method has rapid response, good stability and little influence of ambient temperature, which is suitable for low flow rate flow measurement. The constant power response of low flow rate measurement is relatively slow, the stability is poor, and the influence of ambient temperature is large. It is only suitable for high flow rate gas measurement [11]. Generally, the maximum measurable speed of flow measurement based on the constant power principle is 488 m/s, while the maximum measurable speed of flow measurement based on the constant temperature difference principle can only reach 38 m/s [12, 13]. In the flow controller described in this paper, the measured flow is micro gas flow, that is, the constant temperature working mode is used for flow measurement.

The flow divider in the controller controls the gas flow into the capillary microchannel by designing the flow ratio to ensure that the flow output signal measured by the flow sensor has a linear relationship with the gas flow through the capillary [14]. The total range of the flow controller involved in this article is 3.5 mg/s, and the flow rate through the capillary after being split through the divider is 1.2 mg/s.

3 Fluid Channel Structure Size and Calculation

The structure of the fluid channel involved in this paper is shown in Fig. 2. The inner diameter of the capillary is 0.34 mm, the length is 23 mm. There is a proportional valve downstream to adjust the flow, and the valve opening is 0–10 μm. The fluid working medium is Xe, maximum mass flow is 1.2 mg/s, density is 5.89 kg/m^3, and dynamic viscosity is 0.02110 mPa · s.

Reynolds number:

$$Re = \frac{\rho v d}{\mu} = \frac{Qd}{\mu A} = \frac{4Q}{\pi \mu d} \tag{5}$$

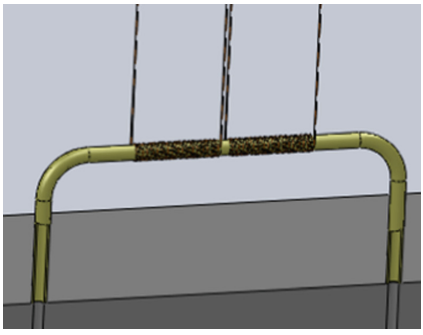

Fig. 2. Schematic Diagram of Fluid Channel Structure

Definition:
v: the average velocity of the fluid, m/s;
ρ: the fluid density, kg/m^3;
μ: dynamic viscosity, Pa · s;
d: Pipe diameter, m.

Calculate the Reynolds number as 213 < 2300, Therefore, the gas flow state in the capillary is laminar flow.

Calculate the length of the heat exchange inlet section:

$$\frac{L}{d} = 0.05Re \tag{6}$$

It is calculated that L = 3.621 mm. So if the length of the inlet section exceeds 3.621 mm, the conditions for sufficient development of flow and heat exchange can be met.

Calculate the Mach number:

$$v = \frac{Q}{\rho d} = 2.25\,\text{m/s} \tag{7}$$

$$Ma = 0.0066 \tag{8}$$

For conventional channels, when the Mach number is less than 0.3, the density change is less than 0.1% when the working pressure changes, and it can be considered as an incompressible fluid. However, for micro-channels, in the supercritical state, the pressure difference between the inlet and the outlet is relatively large, resulting in a relatively obvious change in fluid density; at the same time, the pressure gradient increases, and the full development stage of the flow cannot be quickly reached. Therefore, in the flow analysis and heat transfer analysis It is quite different from the conventional scale channel [15].

When the downstream valve opening is different, the outlet is in a vacuum state, the capillary back pressure will change, the larger the valve opening, the lower the back pressure. Based on Euler differential equations of motion for one-dimensional flow [16]:

$$\frac{\partial V}{\partial t}ds + \frac{dp}{\rho} + VdV + gdz = 0 \tag{9}$$

For the steady flow of gas, if the gravitational potential energy is ignored and the flow parameters do not change with time, the above formula can be simplified as:

$$\frac{dp}{\rho} + VdV = 0 \tag{10}$$

According to Eq. (10), When the pressure decreases, the speed must increase. When the valve opening increases and the valve outlet pressure remains unchanged, the capillary back pressure decreases, resulting in an inevitable increase in fluid velocity. The fluid becomes accelerated in the capillary, rather than the uniform motion after full development. At the same mass flow rate, the fluid density changes, which affects the surface heat transfer coefficient of convective heat transfer between gas and sensor wire. At the same mass flow rate, the measured flow rate is different with different valve opening.

4 Simulation

The above process is simulated and analyzed. Using Fluent, set the inlet working pressure at 0.25 MPa, the outlet is vacuum, the ambient temperature is 30 °C, and the dual winding heating wire is heated at 110 °C. When the mass flow is 1.2 mg/s, the flow velocity distribution, pressure distribution, temperature distribution and heat flux density of different valve openings are simulated respectively, as shown in Figs. 3, 4, 5, 6, 7 and 8. The obtained heating power simulation results for the upstream winding heating section 1 and the downstream winding heating section 2 are shown in Table 1.

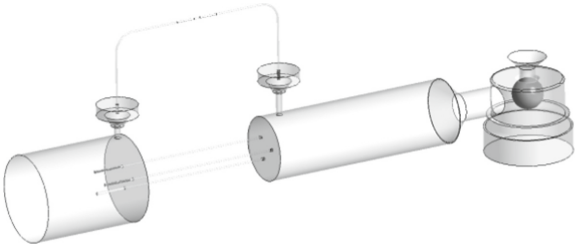

Fig. 3. Computational Domain

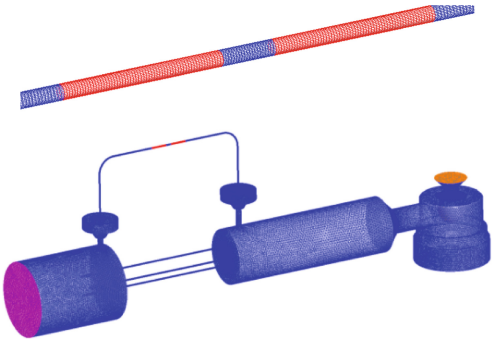

Fig. 4. Grid

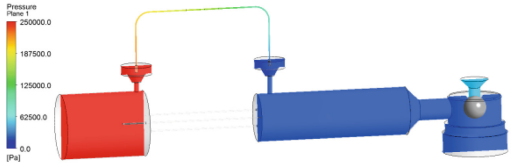

(a) Valve Opening 3μm

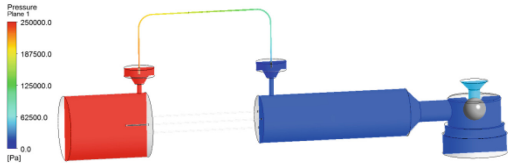

(b) Valve Opening 10μm

Fig. 5. Pressure Distribution in Capillary with Different Valve Openings

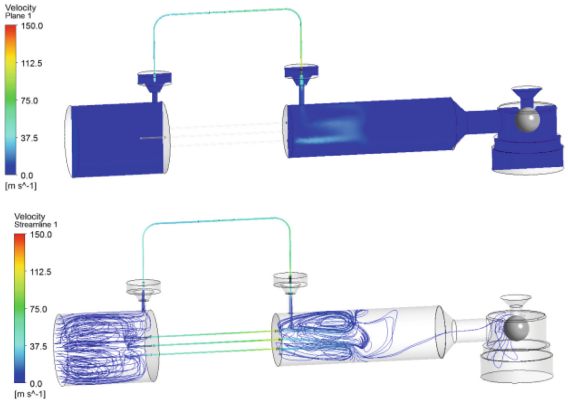

(a) Valve Opening 3μm

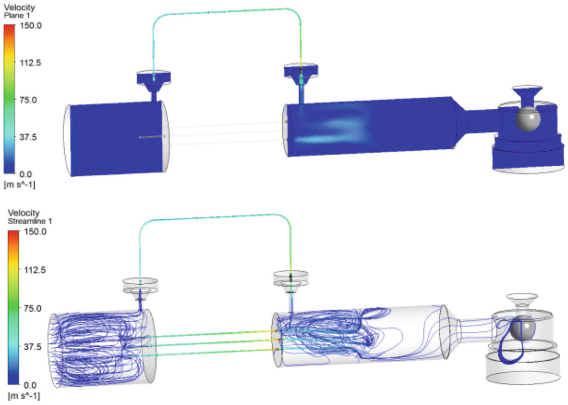

(b) Valve Opening 10μm

Fig. 6. Velocity Distribution in Capillary with Different Valve Opening

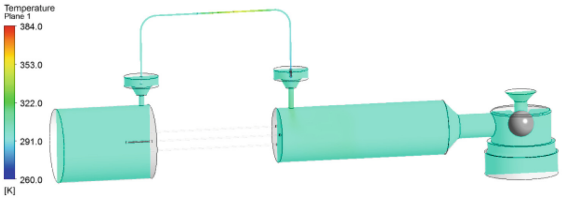

(a) Valve Opening 3μm

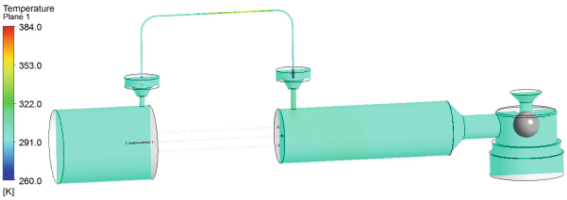

(b) Valve Opening 10μm

Fig. 7. Temperature Distribution in Capillary with Different Valve Opening

Table 1. Heating Power Simulation Results

Valve Opening (μm)	Heating power of the upstream resistor (W)	Heating power of the downstream resistor (W)	Heating Power Difference (W)
3	5.3063E-02	3.2861E-02	2.0202E-02
10	5.8222E-02	3.7196E-02	2.1026E-02

It can be seen from Fig. 5 and Fig. 6 that when the upstream control mass flow rate stays at 1.2 mg/s, when the valve opening is increased from 3 μm to 10 μm, the downstream pressure of the capillary decreases and the flow rate increases. It can be seen from Fig. 7 (a) and (b) that the upstream control mass flow rate is 1.2 mg/s, and the constant temperature mode is set. After the valve opening is increased from 3 μm to 10 μm, the temperature of the upstream and downstream windings remains unchanged, which is always heated to 110 °C. According to Fig. 8 and Table 1, after the valve opening increases, the heat flux density of the upstream winding increases while the heat flux density of the downstream winding decreases. The heating power of both windings is increased, so the measured flow deviates from the actual flow.

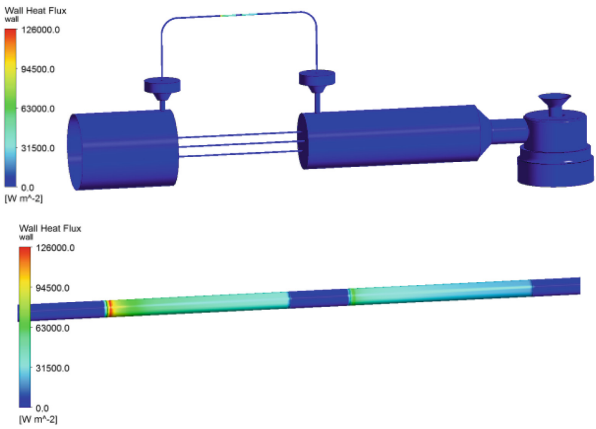

(a) Valve Opening 3μm

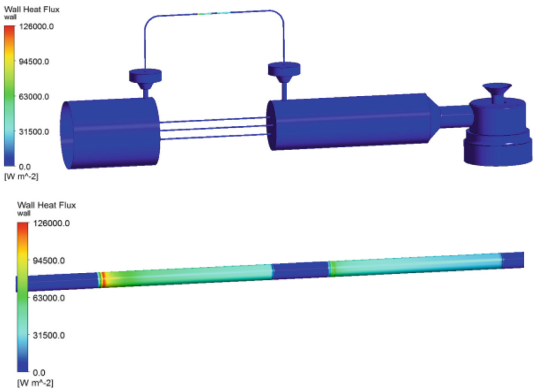

(b) Valve Opening 10μm

Fig. 8. Heat Flux Density in Capillaries with Different Valve Opening

5 Test Verification

In order to verify the influence of different valve opening on flow measurement, a test system was built as shown in Fig. 9. The system includes Xenon gas cylinder, pressure reducer, pressure gauge, pressure controller, gas volume, standard high-precision flowmeter, standard flow controller and vacuum pump. The pressure controller is used to set the working pressure at the product inlet. The standard flowmeter is used to know the actual flow value. Standard flow controller is used to control mass flow. The vacuum pump and gas volume are connected at the downstream of the tested product to keep the outlet of the tested product in an approximate vacuum.

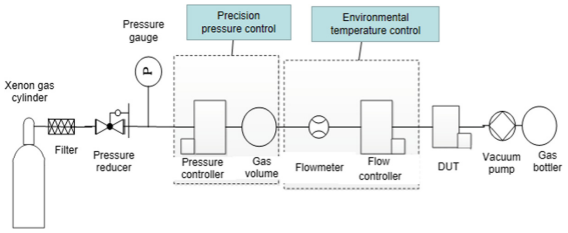

Fig. 9. Test System

Table 2. Test Data

Temperature	Valve Opening 3 μm		Valve Opening 10 μm	
	Product data (10^{-2} W)	Standard flow (mg/s)	Product data (10^{-2} W)	Standard flow (mg/s)
20 °C	2.535	0.000	2.521	0.000
	3.848	0.165	3.846	0.164
	5.192	0.332	5.212	0.330
	6.531	0.498	6.584	0.496
	7.841	0.665	7.931	0.662
	9.088	0.832	9.217	0.829
	10.249	1.000	10.414	0.996
	11.305	1.168	11.500	1.165
30 °C	2.489	0.000	2.417	0.000
	3.802	0.163	3.785	0.165
	5.144	0.328	5.147	0.331
	6.471	0.494	6.518	0.497
	7.763	0.660	7.862	0.664
	8.986	0.826	9.139	0.831
	10.148	0.994	10.323	0.999
	11.185	1.161	11.397	1.167
40 °C	2.440	0.000	2.377	0.000
	3.734	0.166	3.723	0.165
	5.093	0.332	5.089	0.331
	6.433	0.499	6.452	0.497
	7.728	0.665	7.786	0.663
	8.960	0.832	9.050	0.830
	10.113	1.000	10.220	0.997
	11.163	1.169	11.278	1.165

(*continued*)

Table 2. (*continued*)

Temperature	Valve Opening 3 μm		Valve Opening 10 μm	
	Product data (10^{-2} W)	Standard flow (mg/s)	Product data (10^{-2} W)	Standard flow (mg/s)
50 °C	2.297	0.000	2.242	0.000
	3.629	0.165	3.596	0.165
	4.987	0.331	4.972	0.331
	6.327	0.498	6.343	0.498
	7.626	0.665	7.674	0.664
	8.860	0.832	8.934	0.832
	9.993	1.000	10.095	0.999
	11.027	1.168	11.145	1.168

Set the valve on the tested product to a fixed opening, control the mass flow through the upstream standard flow controller, read the mass flow through the standard flowmeter, and conduct flow calibration test. The valve opening is set to 3 μm, 10 μm. The flow rate was tested at 20 °C, 30 °C, 40 °C and 50 °C. The test data are shown in Table 2 and Fig. 10.

According to the above data, when the ambient temperature is the same, after increasing the valve opening, the product output increases under the same mass flow, that is, after the capillary back pressure increases, the fluid acceleration increases the heat exchange between the upstream and downstream windings, and the gas flows through the upstream winding to take away more heat, which increases the heating power of the dual windings, increases the product output, and brings extra measurement errors to the product.

Further analyze the specific data of the above measurement errors. When the valve opening is 10 μm, the least squares method is used to fit the product flow calibration data, and the fitting accuracy is better than ±0.5%FS, as shown in Fig. 11. After reducing the valve opening to 3 μm, substitute the product output data into the fitting formula when the valve opening is 10 μm. The measured actual flow rate and measurement error are shown in Fig. 12. It can be seen that most of the errors are negative errors, and as the flow rate increases, the error increases, and the maximum can reach −3.2%. This error cannot be ignored for flow controller products that require precise regulation of flow.

Therefore, it is necessary to adjust the valve opening to an appropriate value when calibrating flow controller products, to avoid the increase of the calibration flow error.

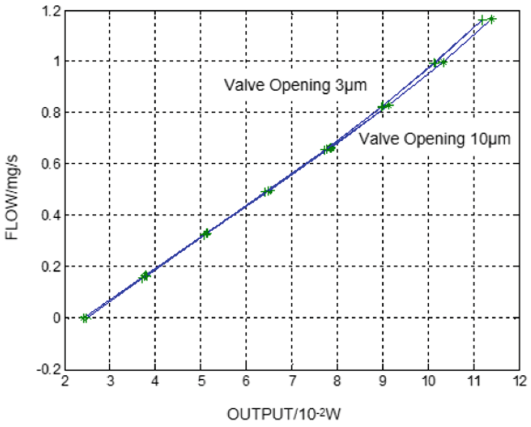

（a）Different Valves Opening at Ambient Temperature of 20 ℃

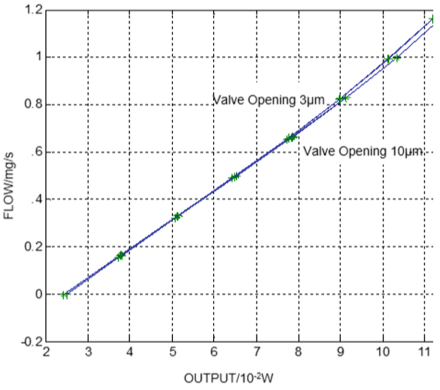

（b）Different Valves Opening at Ambient Temperature of 30 ℃

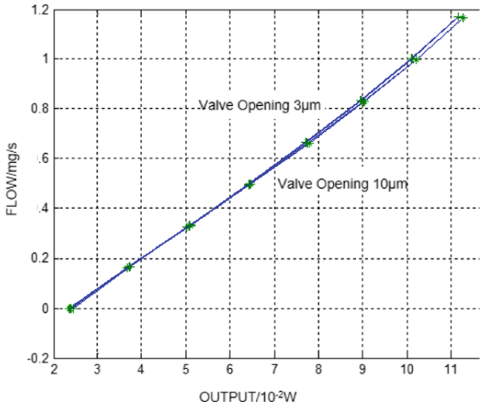

（c）Different Valves Opening at Ambient Temperature of 40 ℃

Fig. 10. Flow Measurement Data When the Valve Opening is Different

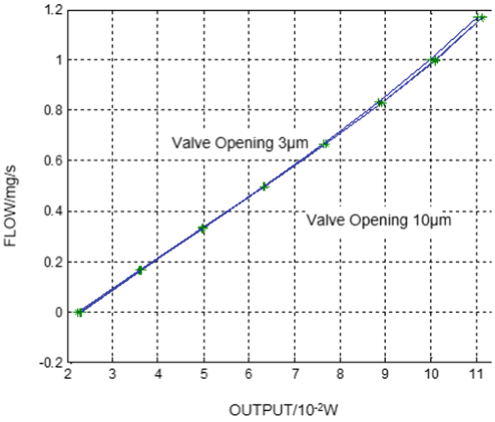

（d）Different Valves Opening at Ambient Temperature of 50 ℃

Fig. 10. (*continued*)

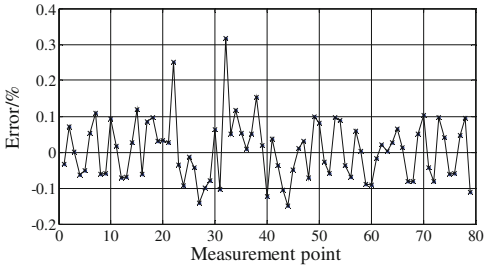

Fig. 11. Fitting Error of flow when the valve opening at 10 μm (less than ±0.5%FS)

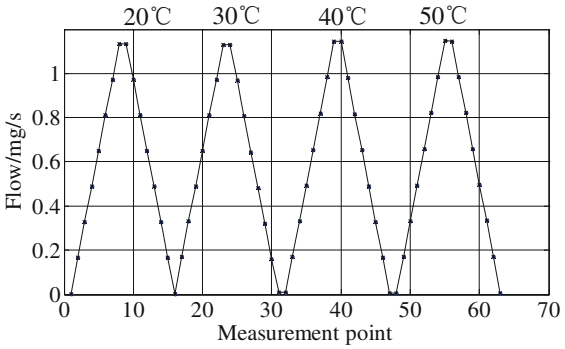

(a) Measured flow rate

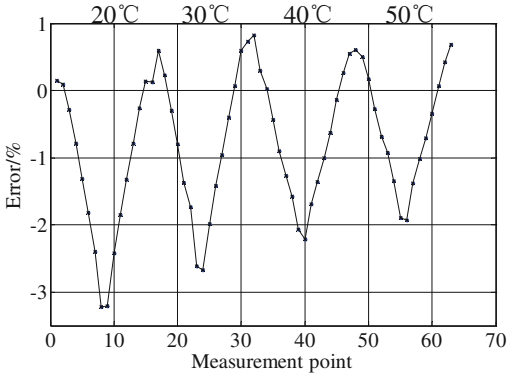

(b) Measurement error

Fig. 12. When the valve opening at 3 μm, the measured flow and Measurement error (Use the fitting formula at 10 μm to calculate the flow)

6 Conclusion

Based on its 0.34 mm capillary microfluidic channel, this paper analyzes the influence of the downstream valve opening on the fluid flow, heat transfer and accurate flow measurement for the flow controller products that are applied to spacecraft and other special working conditions and require precise regulation. The following conclusions are reached:

(1) Under this working condition, the upstream pressure is high and the downstream pressure is almost vacuum. Under the supercritical state, the pressure difference between the inlet and outlet is large, resulting in obvious changes in fluid density, which cannot be simply simplified as incompressible fluid for treatment;
(2) It can be seen from the simulation analysis and experimental data that the larger the opening of valve is, the lower the back pressure of the capillary channel is. Due to the accelerating state of fluid, the fully developed convective heat transfer and

incompressible flow state are damaged, thereby bringing extra measurement error to accurate flow measurement of flow controllers;

(3) In view of this special working condition, it is necessary to use real valves for flow control during calibration test, instead of using standard flow controller to adjust the flow, so that the valve opening of the product is consistent during flow calibration and actual use, that is, the flow measurement error caused by different valve opening can be eliminated.

Acknowledgments. This work was supported by fund project:Key R&D Project of the Ministry of Science and Technology of China (2022YFC2001002).

Authors' Contributions. Conceptualization, Wang Ping and Li Yong; methodology, Fu Xin-ju and Wang Xu-dong; validation, Shi Zhao-xin, Lv Tai-zeng; formal analysis, Wang Ping; investigation, Fu Xin-ju; resources, Fu Xin-ju; data curation, Fu Xin-ju; writing—original draft preparation, Fu Xin-ju; writing—review and editing, Wang Ping; visualization, Wang Xu-dong; supervision, Li Yong; project administration, Fu Xin-ju. All authors have read and agreed to the pub-lished version of the manuscript.

References

1. Wang, X.-D., Li, G.-X., Chen, J., Liu, X.-H., Li, H.-M.: Simulation study on Xeon mass flow regulating characteristics of the proportional valve based on Unimorph ring-shaped piezoelectric actuator. J. Propulsion Technol. **12**, 2867–2873 (2019)
2. Zhao, X.L., Hui, X., Pan, H.P.: Modeling rate-dependent hysteresis in piezoelectric actuators using T-S fuzzy system based on expanded input space method. Sens. Actuators A **283**, 123–127 (2018)
3. Chen, H.X., Zhang, J.Z., Sun, Y.H.: The new generation of thermal mass flowmeter. Process Autom. Instrum. **12**, 33–37 (2009)
4. Silvestri, S., Schena, E.: Micromachined flow sensors in biomedical applications. Micromachines **3**, 225–243 (2012)
5. Armano, M., Audley, H., Baird, J., Binetruy, P., Born, M., Bortoluzzi, D., et al.: LISA pathfinder collaboration. LISA pathfinder micronewton cold gas thrusters: in-flight characterization. Phys. Rev. D **99**(12), 122003 (2019)
6. Wang, X.-D., Li, G.-X., Chen, J., Li, H.-M., Yu, Y.-S.: Simulation study of filling and starting operation characteristics of nitrogen gas micro-propulsion system on a drag-free satellite. J. Astronaut. **11**, 1367–1374 (2019)
7. Zhang, Y.-L., Liu, K., Cheng, M.-S.: Dynamic Theory and Application of Liquid Rocket Engine. Science Press, Bei Jing (2005)
8. Ashauer, M., Glosch, H., Hedrich, F., et al.: Thermal flow sensor for liquids and gases. In: The Eleventh International Workshop on MICRO Electro Mechanical Systems. Mems 98, New York. Proceedings. IEEE, pp. 351–355 (1998)
9. Ashauer, M., Glosch, H., Hedrich, F., et al.: Thermal flow sensor for liquids and gases based on combinations of two principles. Sens. Actuators A **73**(1–2), 7–13 (1999)
10. Su, Q.-Y., Wu, W.: The working principle of thermal gas mass flow sensor. China Instrum. **1**, 62–66 (2017)

11. Mo, R.-J.: Comparison of constant power and constant temperature differential thermal gas mass meters. Autom. Panor. (11), 90–92 (2010)
12. Chen, F., Wang, Z.: Measurement principle and type selection of thermal mass flowmeter. Mod. Metall. (01), 105–108 (2013)
13. Van Honschoten, J.W., Svetovoy, V.B.: Optimization of a thermal flow sensor for acoustic particle velocity measurements. Microelectromech. Syst. 436–443 (2005)
14. Yang, Y.-Q., Yang, G.-H.: The design of the bypass of gas mass flow controller. China Instrum. **5**, 66–69 (2016)
15. Tao, W.-S.: Heat Transfer (Fifth Edition), vol. 7, pp. 261–263. Higher Education Press, Beijing (2019)
16. Wang, X.-Y.: Fundamentals of Aerodynamics, vol. 5, pp. 70–71. Northwestern Polytechnical University Press, Xi'an (2006)